CRYSTAL GROWTH & DESIGN

pubs.acs.org/crystal

Article

Substituent-Controlled Tailoring of Chalcogen-Bonded Supramolecular Nanoribbons in the Solid State

Nicolas Biot, Deborah Romito, and Davide Bonifazi*

Cite This: https://dx.doi.org/10.1021/acs.cgd.0c01318

Read Online

ACCESS | Metrics & More | Article Recommendations | Supporting Information

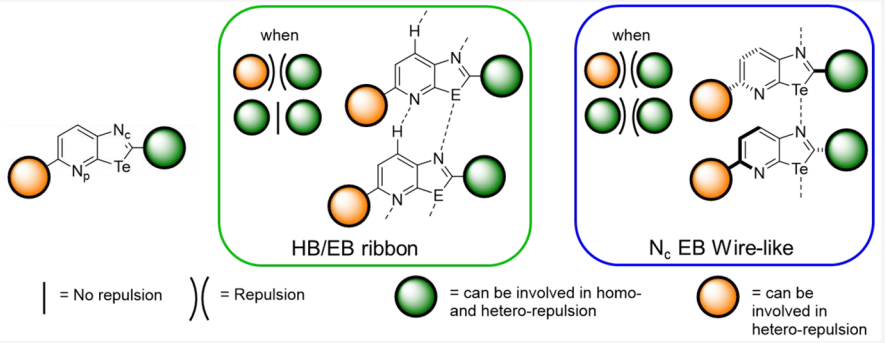

ABSTRACT: In this work, we design and synthesize supramolecular 2,5-substituted chalcogenazolo[5,4-β]pyridine (CGP) synthons arranging in supramolecular ribbons at the solid state. A careful choice of the combination of substituents at the 2- and 5-positions on the CGP scaffold is outlined to accomplish supramolecular materials by means of multiple hybrid interactions, comprising both chalcogen and hydrogen bonds. Depending on the steric and electronic properties of the substituents, different solid-state arrangements have been achieved. Among the different moieties on the 5-position, an oxazole unit has been incorporated on the Se- and Te-congeners by Pd-catalyzed cross-coupling reaction and a supramolecular ribbon-like organization was consistently obtained at the solid state.

INTRODUCTION

In recent years, crystal engineering has soared interest in the scientific community, given its valuable implications in the rational design of functional materials.[1−5] Several studies have focused on the use of supramolecular bonds, selectively involving recognition motifs to generate stable and predictable multidimensional networks in the solid state.[6−10] Among the several noncovalent interactions, hydrogen bonds embody the main interaction occurring in biological systems,[11,12] as well as being used for many applications in chemistry and materials science.[13−16] However, over the past decades, there has been a flourishing interest for a class of exotic noncovalent interactions, namely, Secondary Bonding Interactions (SBIs),[17] as attractive alternatives to the ubiquitous hydrogen bond in crystal engineering. SBIs' nature relies on electrostatic (explained in terms of σ-holes)[18] and van der Waals contributions, as well as on orbital mixing described as $n^2(Y)\rightarrow\sigma^*(E\text{-}X)$ donation (X-E···Y), which involves non-bonding electrons of the electron-donating atom Y and the empty antibonding σ^*_{X-E} located on the E atom.[19] When the central polarizable E atom belongs to Group VI of the periodic table, the term chalcogen bonding (EB, known also as ChB) is used to describe the interaction between a positively polarized chalcogen atom and a Lewis base.[20−22] Despite recent developments in catalysis[23−28] and sensing,[25,29] EB interactions have been mainly exploited in crystal engineering,[30,31] providing a distinctive series of persistent recognition motifs.[32−35] The structure of the most part of these chalcogen-bonding synthons builds on a heterocyclic scaffold, in which the chalcogen bond donors and acceptors are proximal to each other,[36−38] thus effectively developing macrocyclic[39−41] and wire-like[42,43] supramolecular architectures. Previous work done in our group with 2-substituted benzo-1,3-chalcogenazoles described the formation of polymeric structures achieved through single EB interactions.[44,45] When using the chalcogenazolo[5,4-β]pyridine (CGP) module, frontal double chalcogen bonds are obtained in the solid state with high recognition fidelity when the Te chalcogen is used.[46] Notably, changing the derivatization in the 2-position of the CGP ring has allowed the complexity of the molecular assembly to be expanded, engineering organic solids through

Received: September 25, 2020
Revised: November 18, 2020

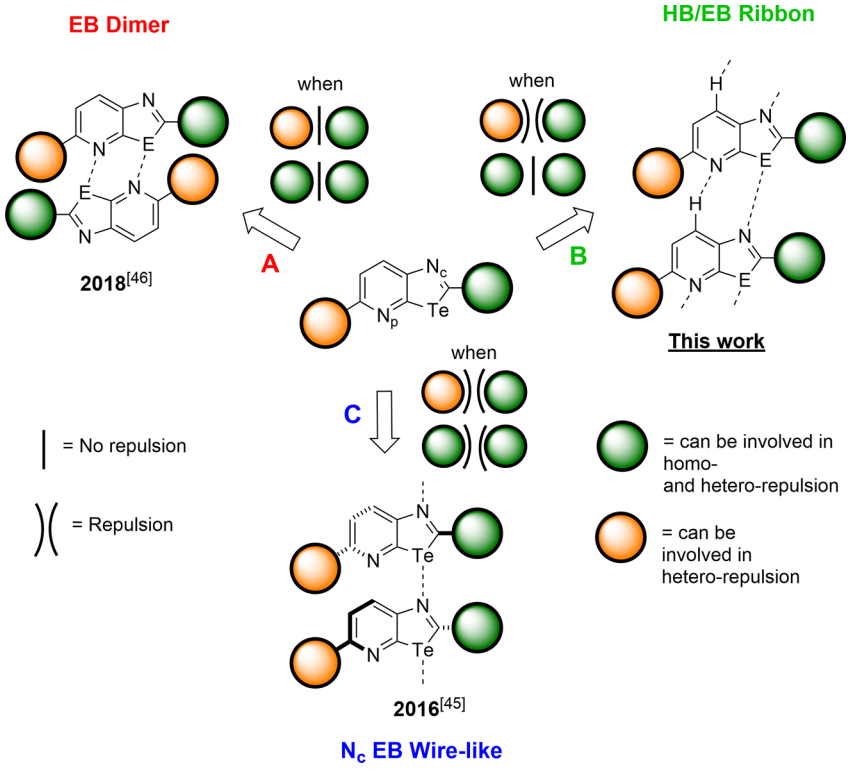

Figure 1. Representation of the design of 2- and 5-substituted CGP scaffold with the recognition modes expected by modulating the repulsive interactions (e.g., steric or electrostatic) between the 2- and the 5-substituents (i.e., green and orange): frontal EB dimers (A), head-to-tail ribbon- (B) and wire-like (C) organizations.

the co-crystallization of heteromolecular supramolecular polymers, held by concurring chalcogen- and halogen-bonding interactions.[47] Building on these results, in this work, we pursue the idea of expanding the functionalization space of the CGP module in the 5-position. This would allow face-to-face dimer association to be disrupted and originate new recognition modes in the solid state (see Figure 1).

Design of 2- and 5-Substituted CGP Derivatives. We conjectured that, depending on the electronic and steric properties of the substituents in the 2- and 5-positions, one could disrupt the typical doubly chalcogen-bonded recognition of a CGP-based derivative (recognition mode A, Figure 1) and force the module to associate in a different fashion. For instance, if the substituent in the 5-position (orange) sterically clashes with that in the 2-position (green) in the frontal arrangement, one could envisage that a head-to-tail recognition mode is favored (e.g., B and C modes displayed in Figure 1). In this arrangement, an EB is established between the N atom of the chalcogenazole ring (N_c) and the chalcogen atom of a neighboring CGP moiety. If no homo-repulsions are present between the substituents in the 2-position (green), a noncovalent ribbon-like organization, held together by a combination of frontal hydrogen- and chalcogen-bonding interactions, is expected to develop (mode B, Figure 1). Finally, if all substituents would undergo homo- and hetero-repulsions in the frontal arrangements, then the only possibility would be for the motif to assemble into nonplanar chalcogen-bonded wire-like assemblies (mode C, Figure 1), as previously observed by us.[45] Aiming at developing synthetically accessible modules with high recognition fidelity, we have focused on the preparation of Te-containing derivatives. Cl, I, and Me groups were chosen as substituents for the 5-position, whereas phenyl, thiophenyl (Th), and CF_3 moieties for the 2-position. To describe the different combinations of substituents in the 2- and 5-positions, the molecules are labeled as **Y-E-R**, where Y stands for the substituent in the 5-position (schematized as an orange sphere, Figure 1), E is the chalcogen atom of interest, and R is the moiety in the 2-position (schematized as a green sphere, Figure 1), respectively.

In our molecular engineering plan, the CGP modules bearing the CF_3 moiety in the 2-position and the bulkiest (Me) and electronegative (Cl) groups in the 5-position (e.g., **Me-Te-CF_3** and **Cl-E-CF_3**) are expected to assemble in a head-to-tail fashion. Similarly, oxazole-bearing **Ox-E-CF_3** is expected to arrange head-to-tail in ribbon-like architectures, with the oxazole ring further strengthening the association through weak H-bonding interactions. On the other hand, when a sizable group is added in the 2-position, the formation of wire-like assemblies is expected (e.g., **Cl-Te-R** and **I-Te-Ph**). Given that repulsive forces originating from the close proximity of the substituents in the self-assembled structure could arise from either steric or electrostatic contributions, electrostatic surface potential (ESP) maps were computed to further understand the contribution of the electrostatic component (see Supporting Information (SI), Table S1 for the calculated $V_{S,max}$ values).

RESULTS AND DISCUSSION

Synthesis. The synthesis started with the selective bromination of the commercially available amines $\mathbf{1}_{Me}$ and $\mathbf{1}_{Cl}$ using *N*-bromo succinimide (NBS) in MeCN, which provided compounds $\mathbf{2}_{Me}$ and $\mathbf{2}_{Cl}$, respectively, in good and excellent yields. Brominated amines $\mathbf{2}_{Me}$ and $\mathbf{2}_{Cl}$ were treated with 1 equiv of *n*-BuLi, followed by the addition of 1 equiv of

https://dx.doi.org/10.1021/acs.cgd.0c01318
Cryst. Growth Des. XXXX, XXX, XXX−XXX

Scheme 1. Synthetic Pathway to 2,5-Functionalized CGP Derivatives[a]

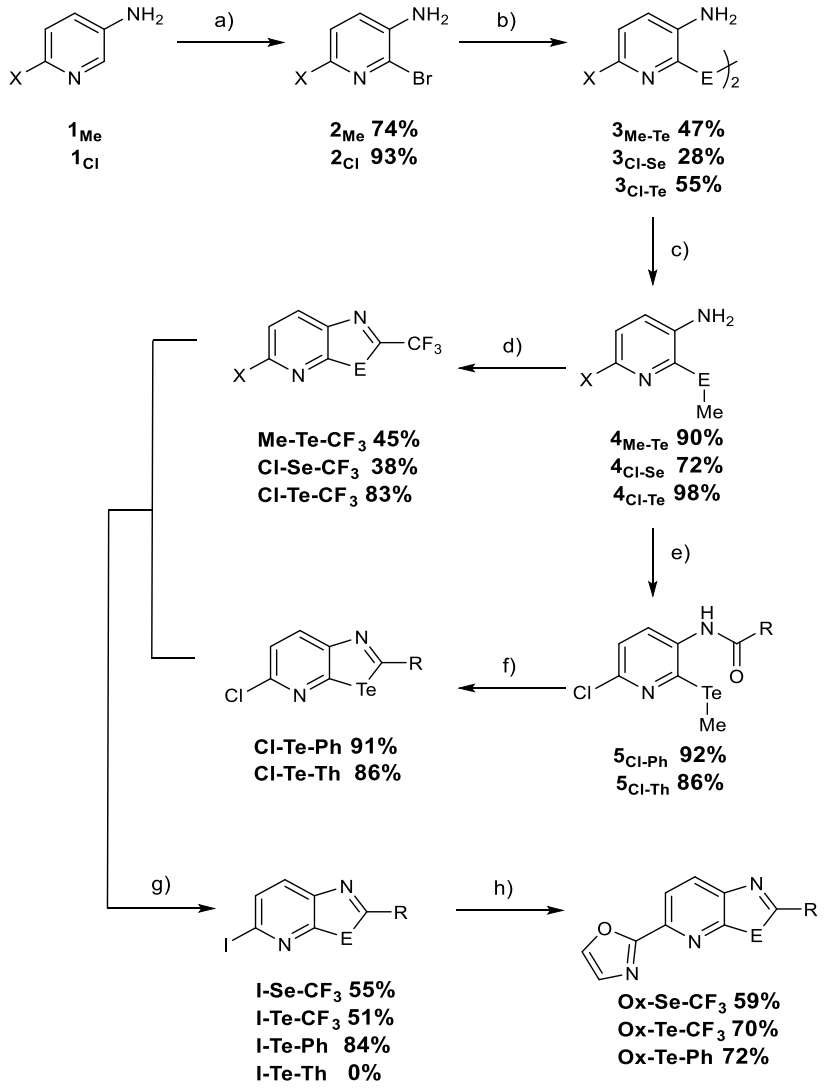

[a]Reagents and conditions: (a) NBS, MeCN, r.t., 5 min; (b) 1. *n*-BuLi, THF, 0 °C, 10 min; 2. *i*-PrBu$_2$MgLi·LiCl, 0 °C, 1 h; 3. E^0, r.t., overnight; 4. Se: $K_3Fe(CN)_6$, H_2O, r.t., 10 min; Te: NH_4Cl, H_2O, air, r.t., 2 h; (c) 1. $NaBH_4$, MeOH, THF, r.t., 1 h; 2. MeI, r.t., 1.5 h; (d) 1. $(CF_3CO)_2O$, CH_2Cl_2, pyridine, 0 °C to r.t., overnight; 2. $POCl_3$, DIPEA, 1,4-dioxane, reflux, overnight; (e) acyl chloride, CH_2Cl_2, pyridine, 0 °C to r.t., overnight; (f) $POCl_3$, DIPEA, 1,4-dioxane, reflux, overnight; (g) AcCl, NaI, MeCN, 80 °C, MW, 12 h; (h) oxazol-2-ylzinc(II) chloride, $[Pd(PPh_3)_4]$ 10 mol %, THF, reflux, 2 h.

trialkyl magnesate (freshly prepared by mixing *i*-PrMgCl with 2 equiv of *n*-BuLi).[48] Subsequent addition of the relevant freshly grounded elemental chalcogen powder to the reaction mixture led to the corresponding bischalcogenides $\mathbf{3_{X\text{-}E}}$ in significantly improved yields (28−55%) when compared to synthetic protocols previously implemented by our group.[46] The synthesis of derivatives $\mathbf{4_{X\text{-}E}}$ was completed by the reductive cleavage of the dichalcogenide bond using $NaBH_4$ and MeOH in THF, followed by addition of MeI. To insert the CF_3 moiety in the 2-position, a one-pot amidation/dehydrative cyclization reaction was performed on $\mathbf{4_{X\text{-}E}}$ using Tf_2O in a 1:1 mixture of CH_2Cl_2 and pyridine, followed by the addition of $POCl_3$ in a 1:1 DIPEA/dioxane solution under refluxing conditions to give **X-E-CF$_3$**. In parallel, Te-bearing amine $\mathbf{4_{Cl\text{-}Te}}$ was converted into amides $\mathbf{5_{Cl\text{-}R}}$ upon reaction with the relevant acyl chloride which, followed by cyclization in the presence of $POCl_3$ in DIPEA and dioxane, afforded **Cl-Te-R** in excellent yields. Given the proved chemical compatibility of the CGP moiety with Pd-catalyzed cross-coupling conditions, a Negishi cross-coupling reaction was attemped to prepare **Ox-Te-Ph** starting from chloro-derivative **Cl-Te-Ph**.[49] Nevertheless, no conversion was observed.

Thus, we moved our attention to the iodo-bearing congeners as electrophilic substrates. As a result, cyclized products bearing chlorine in the 5-position, i.e., **Cl-E-CF$_3$** and **Cl-Te-Ph**, were transformed into iodo-containing **I-E-CF$_3$** and **I-Te-Ph** using NaI in the presence of AcCl in MeCN at 80 °C under microwave irradiation.[50] Finally, reaction between the iodinated derivatives and oxazol-2-ylzinc(II) chloride using $[Pd(PPh_3)_4]$ in THF at reflux afforded targeted molecules **Ox-E-R** in good yields (Scheme 1). All compounds were fully characterized by ^{1}H, ^{19}F, and ^{13}C NMR spectroscopy, IR, mp, and HR-mass spectrometry (see SI).

Solid-State Self-Assembly. The association properties of the 2,5-functionalized CGP derivatives in the solid state were probed by X-ray analysis of single crystals, generally obtained

https://dx.doi.org/10.1021/acs.cgd.0c01318
Cryst. Growth Des. XXXX, XXX, XXX−XXX

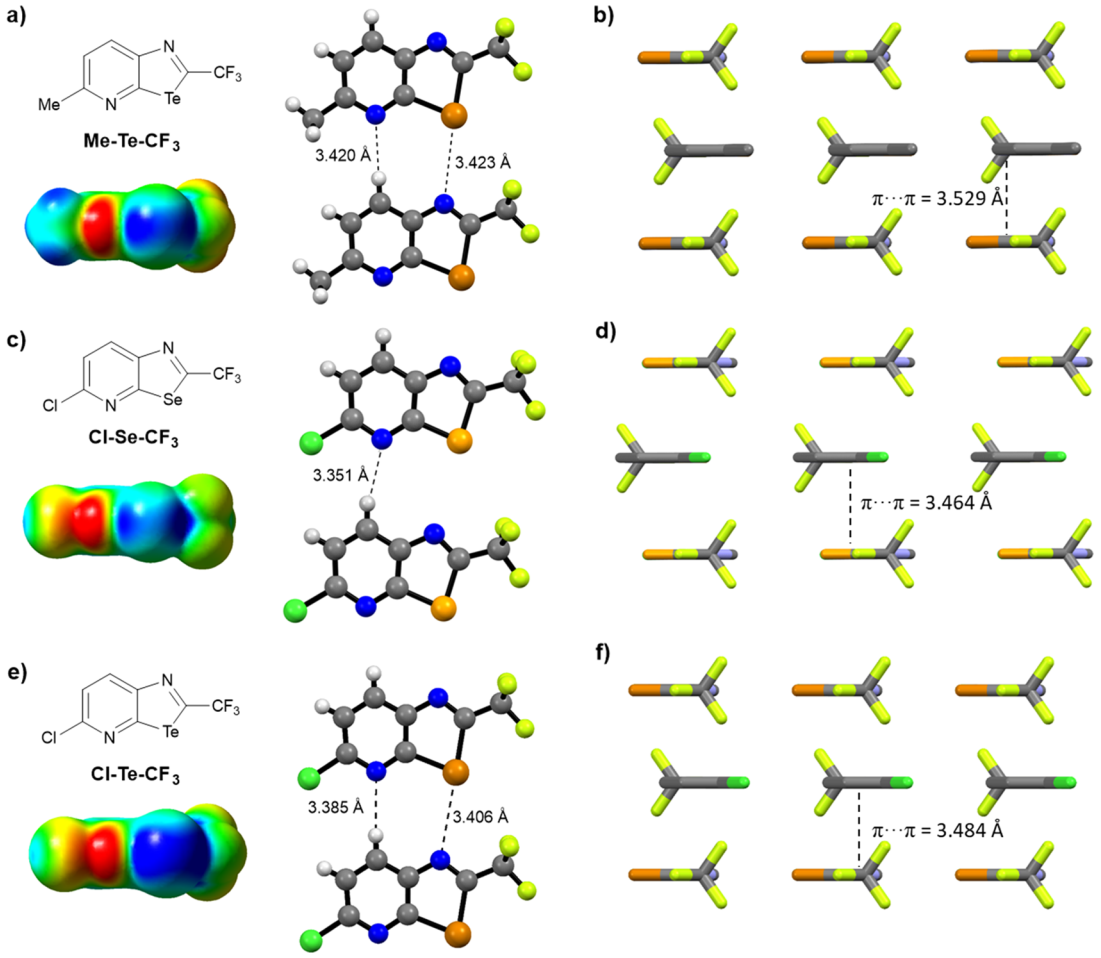

Figure 2. X-ray structures and their respective ESP maps of (a) **Me-Te-CF$_3$**, (c) **Cl-Se-CF$_3$**, and (e) **Cl-Te-CF$_3$**; $\pi-\pi$ stacking arrangements of (b) **Me-Te-CF$_3$**, (d) **Cl-Se-CF$_3$**, and (f) **Cl-Te-CF$_3$**. Space group: $P2_1/m$. Crystallization solvent: $CHCl_3$.

by slow evaporation of a $CHCl_3$ solution. Governed by fluorophilic domains established by the CF_3 moiety in the 2-position, crystals of **Me-Te-CF$_3$** and **Cl-E-CF$_3$** are isomorphs, despite bearing either a Me or Cl atom in the 5-position, either Se or Te atoms. Te-congeners **Me-Te-CF$_3$** (Figure 2a) and **Cl-Te-CF$_3$** (Figure 2e) develop in a ribbon-like arrangement, in which each molecule is involved in frontal interactions comprising a chalcogen bond ($d_{N_c\cdots Te}$ = 3.423 and 3.406 Å for **Me-Te-CF$_3$** and **Cl-Te-CF$_3$**, respectively) and a hydrogen bond, with the latter established between the pyridyl H and N atoms ($d_{N_p\cdots C}$ = 3.420 and 3.385 Å, respectively, for **Me-Te-CF$_3$** and **Cl-Te-CF$_3$**) of two neighboring molecules. Surprisingly, the Se-based congener, **Cl-Se-CF$_3$**, arranges in an analogue ribbon-like orientation (Figure 2c), though held together only by hydrogen-bonding interactions ($d_{N_p\cdots C}$ = 3.351 Å). Additional $\pi-\pi$ stacking interactions, governing the columnar stacking arrangement in a head-to-tail fashion, are also observed ($d_{\pi-\pi}$ = 3.529, 3.464, and 3.484 Å; Figure 2b,d,f respectively), with the longest distance reported for **Me-Te-CF$_3$**. Considering the ESP map of the two different moieties in the 5-position (i.e., depicting the Me group mostly positive and Cl atom mostly negative), one can easily conjecture that the formation of assembly A for **Me-Te-CF$_3$** is hampered by steric repulsion in the case of CF_3 and Me, whereas, in **Cl-Te-CF$_3$**, CF_3 and Cl repel each other through a strong electrostatic component.

Moving to the crystal structure of iodo-derivative **I-Te-CF$_3$**, a different molecular packing could be observed. Interestingly, doubly chalcogen-bonded, distorted noncovalent dimers are observed ($d_{N_p\cdots Te}$ = 3.217 Å). Given the low electronegativity and high polarizability of the I atom, the solid-state arrangement suggests the presence of a weaker repulsion between the CF_3 and I atoms, compared to that between CF_3 and Cl (Figure 3a). Moreover, each dimer associates through double hydrogen bonds involving the N_c atom ($d_{N_c\cdots Te}$ = 3.486 Å), hence generating a kinked ribbon at the solid state (Figure 3b). $\pi-\pi$ stacking interactions are also observed ($d_{\pi-\pi}$ = 3.824 Å with an offset of 2.585 Å), with each column interconnected by multiple halogen bonds ($d_{I\cdots I}$ = 3.482 Å). In this arrangement, each I atom acts simultaneously as both halogen-bonding acceptor and donor (Figure 3c).

As previously observed for compound **Cl-Se-CF$_3$**, also **I-Se-CF$_3$** crystallizes through the formation of ribbon-like structures with no detectable chalcogen-nitrogen contacts. In these crystals, the monomers organize through hydrogen-bonding interaction ($d_{N_p\cdots C}$ = 3.418 Å), which are considerably longer than those observed for **Cl-Se-CF$_3$** (Figure 3d). Notably, **I-Se-CF$_3$** forms columns through $\pi-\pi$ stacking interactions (estimated $d_{\pi-\pi}$ = 3.489 Å), having the CF_3 moieties segregated in fluorinated domains ($d_{F\cdots F}$ = 2.573 and 2.933 Å; Figure 3e). The functionalization of the 2-position with the thiophenyl unit for **Cl-Te-Th** and the phenyl ring for **Cl-Te-**

https://dx.doi.org/10.1021/acs.cgd.0c01318
Cryst. Growth Des. XXXX, XXX, XXX−XXX

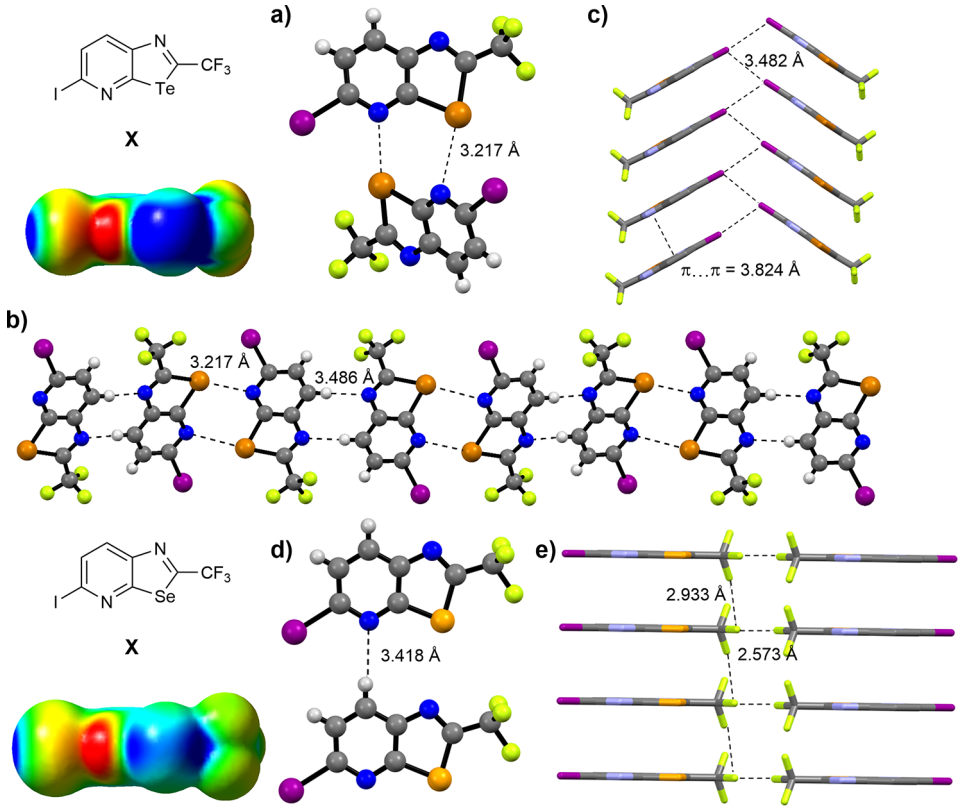

Figure 3. X-ray structures and their ESP maps of (a) **I-Te-CF$_3$** and (d) **I-Se-CF$_3$**; (b) kinked ribbon of **I-Te-CF$_3$**; columnar orientations of (c) **I-Te-CF$_3$** and (e) **I-Se-CF$_3$** (the halogen-bonding and F···F contacts are also displayed). Space groups: *C*2/*c* for **I-Te-CF$_3$**, *Cmca* for **I-Se-CF$_3$**. Crystallization solvent: $CHCl_3$.

Ph and **I-Te-Ph** leads to the growth of wire-like supramolecular structures, held together by single EB between the N_c atom and the Te atom of each neighboring molecule. Notably, the asymmetric unit of compound **Cl-Te-Th** includes two molecules, building a wire-like supramolecular assembly through single EB interactions involving the tellurazole N atom ($d_{N_c\cdots Te}$ = 3.385 Å; Figure 4a). A similar solid-state organization, as that obtained for **Cl-Te-Th**, was observed for **Cl-Te-Ph**. In this case, both Te σ-holes are involved in EB interactions (Figure 4b). Specifically, the σ-hole(α) engages with the tellurazole N_c atom, developing the wire-like arrangement ($d_{N_c\cdots Te}$ = 3.464 Å; Figure 4d), whereas the σ-hole(β) bridges the neighboring supramolecular wires through the interaction with the N_p atom ($d_{N_p\cdots Te}$ = 3.431 Å). Furthermore, the molecules are held together through $\pi-\pi$ stacking interactions in a quasi-parallel fashion (estimated $d_{\pi-\pi}$ = 3.460 Å), with halogen−halogen interactions connecting the columnar architectures ($d_{Cl\cdots Cl}$ = 3.244 Å; Figure 4c). In the case of iodo-derivative **I-Te-Ph**, the asymmetric unit contains two molecules, each interacting with a nearby module through single EB with the N_c atom ($d_{N_c\cdots Te}$ = 3.464 and 3.582 Å). The resulting wire-like organization is further strengthened by weak hydrogen contacts established between the N_p atom and one of the H atoms of the phenyl ring ($d_{N_p\cdots C}$ = 3.237 and 3.321 Å; Figure 4e). In contrast to chlorinated analogue **Cl-Te-Ph**, $\pi-\pi$ stacking interactions govern the formation of columnar arrangements in a quasi-parallel head-to-tail fashion (estimated $d_{\pi-\pi}$ = 3.542 Å), with I···π interactions (σ^*-π, $d_{C\cdots I}$ = 3.505 Å) bridging the columns (Figure 4f).

Building on these observations, one can notice that wire-like structures are consistently attained over ribbon and dimeric arrangements with 5-functionalized CGP modules bearing a phenyl moiety in the 2-position. Remarkably, a shortening of the $N_c\cdots Te$ distance can be observed when passing from phenyl-substituted **Cl-Te-Ph** and **I-Te-Ph** to **Cl-Te-Th**.

Aiming at validating the occurrence of recognition motifs with multiple intermolecular interactions in the solid state, several crystallization attempts for oxazole derivatives **Ox-Te-Ph** and **Ox-E-CF$_3$** have been performed. However, only the CF_3-containing compounds provided single crystals suitable for X-ray diffraction analysis. Notably, Te-congener **Ox-Te-CF$_3$** develops HB/EB ribbons in the solid state. These structures differentiate from those described so far because the O atom of the oxazole and the N atom of the pyridyl moiety both engage in two hydrogen bonds with the H atoms in positions 6 and 7 of a neighboring molecule ($d_{O\cdots C}$ = 3.211 Å and $d_{N\cdots C}$ = 3.423 Å, respectively). A frontal chalcogen bond is also established between the N_c and Te atoms of two adjacent molecules ($d_{N_c\cdots Te}$ = 3.355 Å; Figure 5a). Considering that the length of this EB is shorter ($d_{N_c\cdots Te}$ = 3.355 Å) than those found in the crystal structures of **Me-Te-CF$_3$** and **Cl-Te-CF$_3$** ($d_{N_c\cdots Te}$ = 3.423 and 3.406 Å, respectively), it is suggested that two HB interactions synergistically strengthen the association between the two molecular modules. Supplementary $\pi-\pi$ stacking interactions can be discerned in the molecular packing ($d_{\pi-\pi}$ = 3.392 Å; Figure 5b), with each molecular module arranged in an antiparallel fashion. An analogue supramolecular organization is observed for Se-based congener **Ox-Se-CF$_3$**, having the O atom involved in a hydrogen bond,

https://dx.doi.org/10.1021/acs.cgd.0c01318
Cryst. Growth Des. XXXX, XXX, XXX−XXX

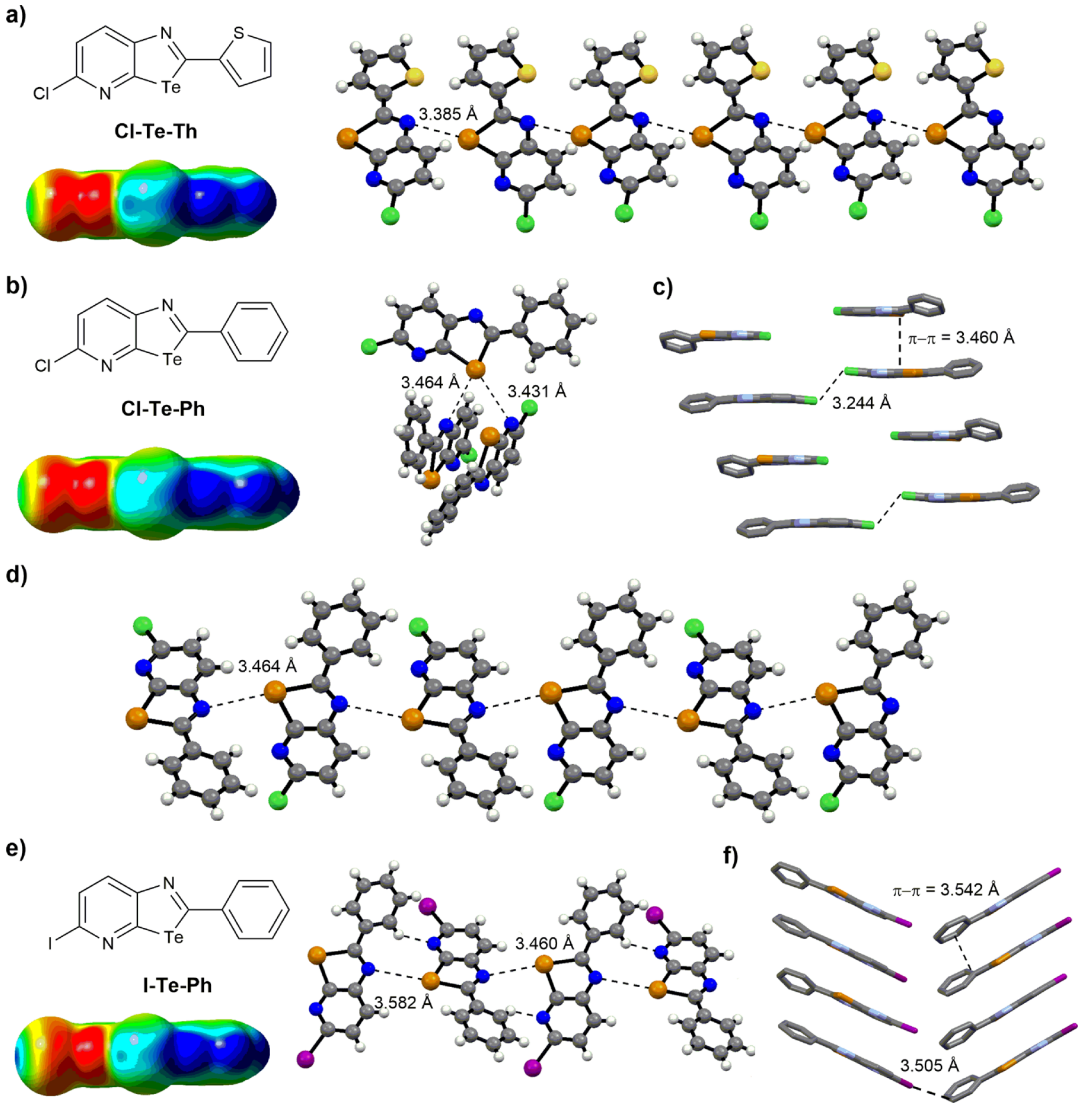

Figure 4. X-ray structures and their ESP maps of (a) **Cl-Te-Th** and (b) **Cl-Te-Ph**, chalcogen bonds are highlighted; wire-like supramolecular architectures of (d) **Cl-Te-Ph** and (e) **I-Te-Ph**; stick representation of columnar arrangements of (c) **Cl-Te-Ph** and (f) **I-Te-Ph**, with $\pi-\pi$ stacking and halogen-bonding interactions highlighted. H atoms are omitted for clarity. Space groups: *Pbac* for **I-Te-Ph**, $P2_1/c$ for **Cl-Te-Th** and **Cl-Te-Ph**. Crystallization solvent: $CHCl_3$.

as well as the N_p atom, with the H atoms in 6- and 7-positions of the facing molecular neighbor ($d_{O\cdots C}$ = 3.201 Å, $d_{N_p\cdots C}$ = 3.418 Å). This governs the arrangement of the synthons in ribbons at the solid state (Figure 5c). Similarly to **Cl-Se-CF$_3$** and **I-Se-CF$_3$**, no chalcogen bond could be observed for **Ox-Se-CF$_3$**, given that the Se···N distance was longer than the sum of their van der Waals radii ($d_{N_c\cdots Se}$ = 3.514 Å > 3.45 Å). In addition, the crystal packing develops through antiparallel $\pi-\pi$ stacking ($d_{\pi-\pi}$ = 3.369 Å; Figure 5d).

CONCLUSIONS

In this paper, we have expanded the recognition space of the CGP moiety in the solid state. By combining the substituents in positions 2 (phenyl, thiophenyl, and CF_3 moieties) and 5 (Me group, Cl and I atoms), a large variety of supramolecular assemblies in the solid state could be obtained by modulating the substituents' steric and electronic properties. Aiming at developing a recognition pattern based on multiple HB and simultaneous single EB interactions, oxazolyl-bearing CGP molecules **Ox-Te-CF$_3$** and **Ox-Se-CF$_3$** have been prepared, with the latter used as reference compound to study the role of the chosen chalcogen atom in the new recognition systems. As expected, the choice of a small moiety as CF_3 in the 2-position, combined with Me, Cl, and oxazole substituents in the 5-position, governed the formation of supramolecular head-to-tail HB/EB ribbons. Replacing Cl with an I atom in the 5-position in Te-congener **I-Te-CF$_3$** led to the formation of distorted EB dimers, arranged into a kinked ribbon in the solid state. Furthermore, derivatives bearing sterically demanding phenyl and thiophenyl groups showed the typical wiring organization. These results could open the road toward the engineering of a large variety of materials marked by tunable molecular arrangements, as well as depicting heteromolecular recognition systems involving HB and EB interactions. The encoding of concomitant weak interactions at the solid state could allow the design of multiresponsive materials for applications in optoelectronics and sensing.

https://dx.doi.org/10.1021/acs.cgd.0c01318
Cryst. Growth Des. XXXX, XXX, XXX−XXX

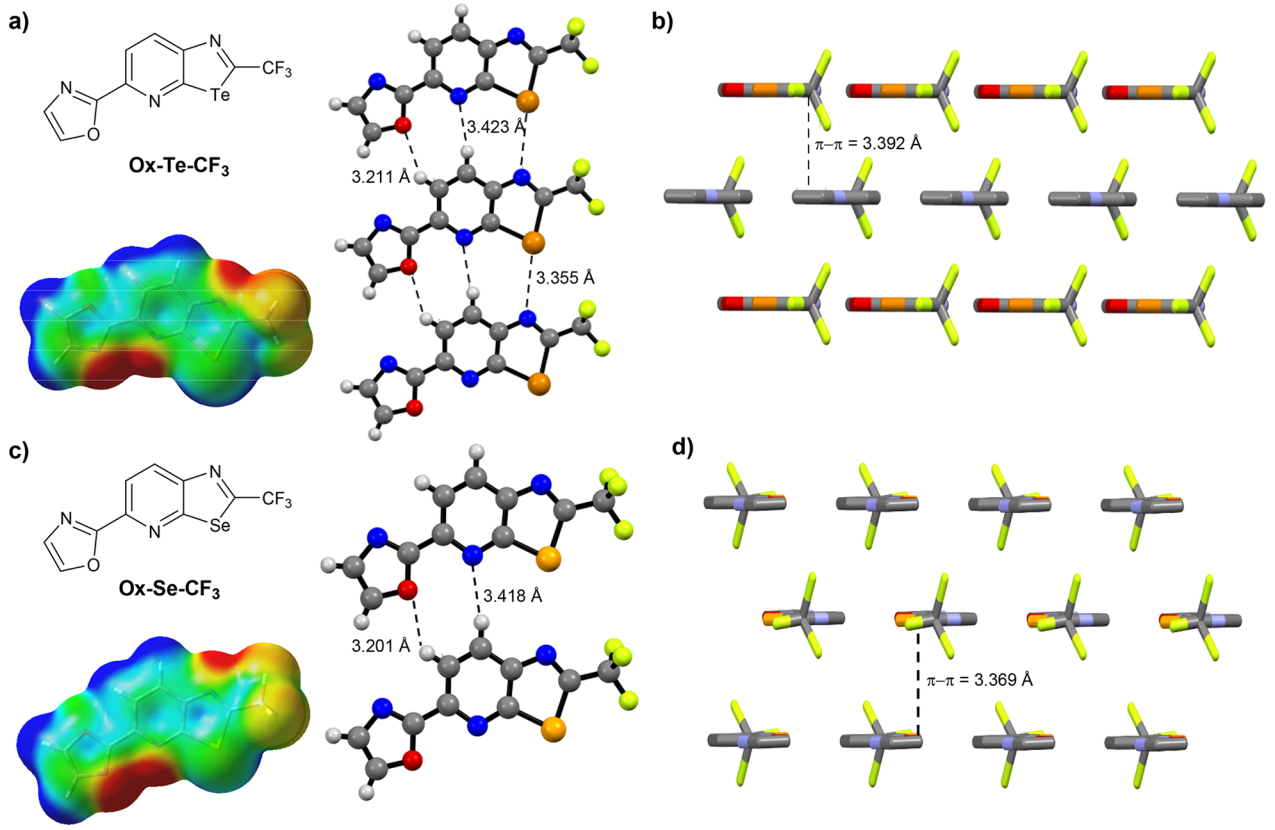

Figure 5. X-ray structures and their ESP maps of (a) **Ox-Te-CF$_3$** and (c) **Ox-Se-CF$_3$**; stick representation of the π–π stacking of (b) **Ox-Te-CF$_3$** and (d) **Ox-Se-CF$_3$**. H atoms are omitted for clarity. Space groups: *Pnma* for **Ox-Te-CF$_3$**, $P2_1/c$ for **Ox-Se-CF$_3$**. Crystallization solvents: EtOH for **Ox-Te-CF$_3$**, C_6H_6 for **Ox-Se-CF$_3$**.

■ ASSOCIATED CONTENT

Supporting Information

The Supporting Information is available free of charge at https://pubs.acs.org/doi/10.1021/acs.cgd.0c01318.

Synthetic protocols and spectroscopic data for all molecules, computational studies, X-ray data (PDF)

Accession Codes

CCDC 1954271, 1954273–1954278, and 2015556–2015558 contain the supplementary crystallographic data for this paper. These data can be obtained free of charge via www.ccdc.cam.ac.uk/data_request/cif, or by emailing data_request@ccdc.cam.ac.uk, or by contacting The Cambridge Crystallographic Data Centre, 12 Union Road, Cambridge CB2 1EZ, UK; fax: +44 1223 336033.

■ AUTHOR INFORMATION

Corresponding Author

Davide Bonifazi − *Institute of Organic Chemistry, University of Vienna, 1090 Vienna, Austria;* orcid.org/0000-0001-5717-0121; Email: davide.bonifazi@univie.ac.at

Authors

Nicolas Biot − *School of Chemistry, Cardiff University, CF10 3AT Cardiff, United Kingdom*

Deborah Romito − *Institute of Organic Chemistry, University of Vienna, 1090 Vienna, Austria*

Complete contact information is available at: https://pubs.acs.org/10.1021/acs.cgd.0c01318

Notes

The authors declare no competing financial interest.

■ ACKNOWLEDGMENTS

D.B. gratefully acknowledges Cardiff University, the University of Vienna, and the EU through the MSCA-RISE funding scheme (project INFUSION) for the financial support. The authors also acknowledge the use of the Advanced Computing (ARCCA) at Cardiff University, and associated support services for the theoretical calculations.

■ REFERENCES

(1) Desiraju, G. R.; Parshall, G. W. Crystal engineering: the design of organic solids. *Mater. Sci. Monogr.* **1989**, *54*, 312–326.

(2) Braga, D.; Desiraju, G. R.; Miller, J. S.; Orpen, A. G.; Price, S. L. Innovation in crystal engineering. *CrystEngComm* **2002**, *4*, 500–509.

(3) Whitesides, G. M.; Grzybowski, B. Self-Assembly at All Scales. *Science* **2002**, *295*, 2418–2421.

(4) Tiekink, E. R.; Vittal, J. *Frontiers in crystal engineering*; John Wiley & Sons, 2006.

(5) Desiraju, G. R. Crystal engineering: a holistic view. *Angew. Chem., Int. Ed.* **2007**, *46*, 8342–8356.

(6) Lehn, J. M. Supramolecular chemistry: from molecular information towards self-organization and complex matter. *Rep. Prog. Phys.* **2004**, *67*, 249.

(7) Badjić, J. D.; Nelson, A.; Cantrill, S. J.; Turnbull, W. B.; Stoddart, J. F. Multivalency and cooperativity in supramolecular chemistry. *Acc. Chem. Res.* **2005**, *38*, 723–732.

(8) Lehn, J. M. From supramolecular chemistry towards constitutional dynamic chemistry and adaptive chemistry. *Chem. Soc. Rev.* **2007**, *36*, 151–160.

(9) Lehn, J. M. Towards complex matter: supramolecular chemistry and self-organization. *European Review* **2009**, *17*, 263−280.
(10) Stupp, S. I.; Palmer, L. C. Supramolecular chemistry and self-assembly in organic materials design. *Chem. Mater.* **2014**, *26*, 507−518.
(11) Sarkhel, S.; Desiraju, G. R. N-H···O, O-H···O, and C-H···O hydrogen bonds in protein−ligand complexes: Strong and weak interactions in molecular recognition. *Proteins: Struct., Funct., Genet.* **2004**, *54*, 247−259.
(12) Sivakova, S.; Rowan, S. J. Nucleobases as supramolecular motifs. *Chem. Soc. Rev.* **2005**, *34*, 9−21.
(13) Wilson, A. J. Non-covalent polymer assembly using arrays of hydrogen-bonds. *Soft Matter* **2007**, *3*, 409−425.
(14) Medhekar, N. V.; Ramasubramaniam, A.; Ruoff, R. S.; Shenoy, V. B. Hydrogen bond networks in graphene oxide composite paper: structure and mechanical properties. *ACS Nano* **2010**, *4*, 2300−2306.
(15) Herbst, S.; Soberats, B.; Leowanawat, P.; Lehmann, M.; Würthner, F. A Columnar Liquid-Crystal Phase Formed by Hydrogen-Bonded Perylene Bisimide J-Aggregates. *Angew. Chem.* **2017**, *129*, 2194−2197.
(16) Du, X.; Lu, X.; Zhao, J.; Zhang, Y.; Li, X.; Lin, H.; Zheng, C.; Tao, S. Hydrogen bond induced green solvent processed high performance ternary organic solar cells with good tolerance on film thickness and blend ratios. *Adv. Funct. Mater.* **2019**, *29*, 1902078.
(17) Alcock, N. W. In *Advances in Inorganic Chemistry and Radiochemistry*, Vol. *15*; Elsevier, 1972; pp 1−58.
(18) Politzer, P.; Murray, J. S.; Clark, T. Halogen bonding and other σ-hole interactions: a perspective. *Phys. Chem. Chem. Phys.* **2013**, *15*, 11178−11189.
(19) Cozzolino, A. F.; Elder, P. J. W.; Vargas-Baca, I. A survey of tellurium-centered secondary-bonding supramolecular synthons. *Coord. Chem. Rev.* **2011**, *255*, 1426−1438.
(20) Werz, D. B.; Gleiter, R.; Rominger, F. Nanotube formation favored by chalcogen−chalcogen interactions. *J. Am. Chem. Soc.* **2002**, *124*, 10638−10639.
(21) Pascoe, D. J.; Ling, K. B.; Cockroft, S. L. The origin of chalcogen-bonding interactions. *J. Am. Chem. Soc.* **2017**, *139*, 15160−15167.
(22) Aakeroy, C. B.; Bryce, D. L.; Desiraju, G. R.; Frontera, A.; Legon, A. C.; Nicotra, F.; Rissanen, K.; Scheiner, S.; Terraneo, G.; Metrangolo, P.; Resnati, G. Definition of the chalcogen bond (IUPAC Recommendations 2019). *Pure Appl. Chem.* **2019**, *91*, 1889−1892.
(23) Wonner, P.; Vogel, L.; Düser, M.; Gomes, L.; Kniep, F.; Mallick, B.; Werz, D. B.; Huber, S. M. Carbon−Halogen Bond Activation by Selenium-Based Chalcogen Bonding. *Angew. Chem., Int. Ed.* **2017**, *56*, 12009−12012.
(24) Benz, S.; Besnard, C.; Matile, S. Chalcogen-Bonding Catalysis: From Neutral to Cationic Benzodiselenazole Scaffolds. *Helv. Chim. Acta* **2018**, *101*, e1800075.
(25) Vogel, L.; Wonner, P.; Huber, S. M. Chalcogen bonding: An overview. *Angew. Chem., Int. Ed.* **2019**, *58*, 1880−1891.
(26) Wonner, P.; Dreger, A.; Vogel, L.; Engelage, E.; Huber, S. M. Chalcogen Bonding Catalysis of a Nitro-Michael Reaction. *Angew. Chem., Int. Ed.* **2019**, *58*, 16923−16927.
(27) Macchione, M.; Goujon, A.; Strakova, K.; Humeniuk, H. V.; Licari, G.; Tajkhorshid, E.; Sakai, N.; Matile, S. A Chalcogen-Bonding Cascade Switch for Planarizable Push−Pull Probes. *Angew. Chem.* **2019**, *131*, 15899−15903.
(28) Young, C. M.; Elmi, A.; Pascoe, D. J.; Morris, R. K.; McLaughlin, C.; Woods, A. M.; Frost, A. B.; De La Houpliere, A.; Ling, K. B.; Smith, T. K.; Slawin, A. M. Z.; Willoughby, P. H.; Cockroft, S. L.; Smith, A. D. The Importance of 1,5-Oxygen··· Chalcogen Interactions in Enantioselective Isochalcogenourea Catalysis. *Angew. Chem.* **2020**, *132*, 3734−3739.
(29) Bamberger, J.; Ostler, F.; Mancheño, O. G. Frontiers in Halogen and Chalcogen-Bond Donor Organocatalysis. *ChemCatChem* **2019**, *11*, 5198−5211.
(30) Fanfrlík, J.; Přáda, A.; Padělková, Z.; Pecina, A.; Macháček, J.; Lepšík, M.; Holub, J.; Růžička, A.; Hnyk, D.; Hobza, P. The dominant role of chalcogen bonding in the crystal packing of 2D/3D aromatics. *Angew. Chem.* **2014**, *126*, 10303−10306.
(31) Scilabra, P.; Terraneo, G.; Resnati, G. The chalcogen bond in crystalline solids: A world parallel to halogen bond. *Acc. Chem. Res.* **2019**, *52*, 1313−1324.
(32) Chivers, T.; Laitinen, R. S. Tellurium: a maverick among the chalcogens. *Chem. Soc. Rev.* **2015**, *44*, 1725−1739.
(33) Mahmudov, K. T.; Kopylovich, M. N.; Guedes da Silva, M. F. C.; Pombeiro, A. J. L. Chalcogen bonding in synthesis, catalysis and design of materials. *Dalton Trans.* **2017**, *46*, 10121−10138.
(34) Ho, P. C.; Wang, J. Z.; Meloni, F.; Vargas-Baca, I. Chalcogen bonding in materials chemistry. *Coord. Chem. Rev.* **2020**, *422*, 213464.
(35) Biot, N.; Bonifazi, D. Chalcogen-bond driven molecular recognition at work. *Coord. Chem. Rev.* **2020**, *413*, 213243.
(36) Cozzolino, A. F.; Vargas-Baca, I.; Mansour, S.; Mahmoudkhani, A. H. The nature of the supramolecular association of 1, 2, 5-chalcogenadiazoles. *J. Am. Chem. Soc.* **2005**, *127*, 3184−3190.
(37) Pati, P. B.; Zade, S. S. Benzoselenadiazole containing donor−acceptor−donor small molecules: nonbonding interactions, packing patterns, and optoelectronic properties. *Cryst. Growth Des.* **2014**, *14*, 1695−1700.
(38) Kumar, V.; Xu, Y.; Leroy, C.; Bryce, D. L. Direct investigation of chalcogen bonds by multinuclear solid-state magnetic resonance and vibrational spectroscopy. *Phys. Chem. Chem. Phys.* **2020**, *22*, 3817−3824.
(39) Ho, P. C.; Szydlowski, P.; Sinclair, J.; Elder, P. J.; Kübel, J.; Gendy, C.; Lee, L. M.; Jenkins, H.; Britten, J. F.; Morim, D. R.; Vargas-Baca, I. Supramolecular macrocycles reversibly assembled by Te···O chalcogen bonding. *Nat. Commun.* **2016**, *7*, 11299.
(40) Ho, P. C.; Rafique, J.; Lee, J.; Lee, L. M.; Jenkins, H. A.; Britten, J. F.; Braga, A. L.; Vargas-Baca, I. Synthesis and structural characterisation of the aggregates of benzo-1, 2-chalcogenazole 2-oxides. *Dalton Trans.* **2017**, *46*, 6570−6579.
(41) Riwar, L. J.; Trapp, N.; Root, K.; Zenobi, R.; Diederich, F. Supramolecular capsules: strong versus weak chalcogen bonding. *Angew. Chem., Int. Ed.* **2018**, *57*, 17259−17264.
(42) Huynh, H. T.; Jeannin, O.; Fourmigué, M. Organic selenocyanates as strong and directional chalcogen bond donors for crystal engineering. *Chem. Commun.* **2017**, *53*, 8467−8469.
(43) Ams, M. R.; Trapp, N.; Schwab, A.; Milić, J. V.; Diederich, F. Chalcogen bonding "2S−2N squares" versus competing interactions: Exploring the recognition properties of sulfur. *Chem. - Eur. J.* **2019**, *25*, 323−333.
(44) Kremer, A.; Aurisicchio, C.; De Leo, F.; Ventura, B.; Wouters, J.; Armaroli, N.; Barbieri, A.; Bonifazi, D. Walking down the chalcogenic group of the periodic table: from singlet to triplet organic emitters. *Chem. - Eur. J.* **2015**, *21*, 15377−15387.
(45) Kremer, A.; Fermi, A.; Biot, N.; Wouters, J.; Bonifazi, D. Supramolecular Wiring of Benzo-1,3-chalcogenazoles through Programmed Chalcogen Bonding Interactions. *Chem. - Eur. J.* **2016**, *22*, 5665−5675.
(46) Biot, N.; Bonifazi, D. Programming Recognition Arrays through Double Chalcogen-Bonding Interactions. *Chem. - Eur. J.* **2018**, *24*, 5439−5443.
(47) Biot, N.; Bonifazi, D. Concurring Chalcogen- and halogen-bonding interactions in supramolecular polymers for crystal engineering applications. *Chem. - Eur. J.* **2020**, *26*, 2904−2913.
(48) Inoue, A.; Kitagawa, K.; Shinokubo, H.; Oshima, K. Selective Halogen−Magnesium Exchange Reaction via Organomagnesium Ate Complex. *J. Org. Chem.* **2001**, *66*, 4333−4339.
(49) Romito, D.; Biot, N.; Babudri, F.; Bonifazi, D. Non-covalent bridging of bithiophenes through chalcogen bonding grips. *New J. Chem.* **2020**, *44*, 6732−6738.
(50) Bissember, A. C.; Banwell, M. G. Microwave-assisted trans-halogenation reactions of various chloro-, bromo-, trifluoromethanesulfonyloxy- and nonafluorobutanesulfonyloxy-substituted quinolines, isoquinolines, and pyridines leading to the corresponding iodinated heterocycles. *J. Org. Chem.* **2009**, *74*, 4893−4895.

https://dx.doi.org/10.1021/acs.cgd.0c01318
Cryst. Growth Des. XXXX, XXX, XXX−XXX